

A Joint Scheme of Antenna Placement and Power Allocation in a Compressive Sensing-Based Colocated MIMO Radar

Abollah Ajorloo¹, Arash Amini^{1*}, and Rouhollah Amiri¹

¹Electrical Engineering Department, Sharif University of Technology, Tehran, Iran

*Senior Member, IEEE

Manuscript received xxxx xx, 202x; revised xxxx xx, 202x; accepted xxxx xx, 202x. Date of publication xxxx xx, 202x; date of current version xxxx xx, 202x.

Abstract—The spatial sparsity of targets in the radar scene is widely used in multiple-input multiple-output (MIMO) radar signal processing, either to improve the detection/estimation performance of the radar or to reduce the cost of the conventional MIMO radars (e.g. by reducing the number of antennas). While sparse target estimation is the main challenge in such an approach, here we address the design of a compressive sensing-based MIMO radar which facilitates such estimations. In particular, we propose an efficient solution for the problem of joint power allocation and antenna placement based on minimizing the number of transmit antennas while constraining the coherence of the sensing matrix. Numerical results confirm the superiority of the proposed method over the existing ones.

Index Terms—Colocated MIMO radar, compressive sensing, antenna placement, power allocation.

I. INTRODUCTION

Multiple-input multiple-output (MIMO) radar systems have been the focus of extensive research in the last decade as they are known to provide superior performances compared to the conventional radars [1], [2]. Based on the antenna configuration, MIMO radars are generally categorized as either colocated [1] or widely separated [2]. In this paper, we consider colocated MIMO radars that have superior parameter identifiability, spatial resolution and interference rejection.

Due to the spatial sparsity of the radar scene, the techniques in compressive sensing (CS) and in particular, sparse recovery methods are found to be very efficient for multi-target detection/estimation in MIMO radars [3], [4]. The success of sparse recovery methods, besides the sparsity level of the radar scene, depends on the properties of the associated sensing matrix. This matrix, describes how the sparse targets are represented in the measured data. The restricted isometry property (RIP) is a well-known sufficient condition that guarantees the stability of sparse recovery methods in noisy settings [5]. Unfortunately, the verification of RIP for a given matrix is computationally NP-hard and infeasible in practice. The mutual coherence of the sensing matrix is a common alternative to guarantee the performance of sparse recovery methods in a worst-case scenario. Computationally, the evaluation of mutual coherence is possible for a wide range of matrix sizes, which makes it one of the popular tools for designing and modifying sensing matrices [4], [6], [7].

There exist several research studies on the design of CS-based colocated MIMO radars in recent years [8]–[15]. Power allocation and waveform design schemes for CS-based colocated MIMO radars with arbitrary given locations of antennas have been addressed in [8]–[11]. While [8], [9] attempt to make the gram matrix of the sensing

matrix as close as possible to identity matrix, the coherence of the sensing matrix is directly minimized in [10], [11]. A sparsity-aware design for the transmitting beam pattern of a frequency diverse array (FDA) MIMO radar is proposed in [12]. Again, the mutual coherence of the sensing matrix is minimized so as to achieve high-resolution estimation in both range and angle. We should highlight that designing a low-cost MIMO radar that meets the performance requirements with a reduced number of antennas is highly desirable. Such antenna reductions can be achieved by exploiting the available degrees of freedom (DOFs) in placement of the antenna elements (in contrast to the conventional equi-spaced linear arrays)[13]. In this regard, there are also a few random placement methods such as [14], [15] with statistical guarantees for sparse recovery performance. Aside from the array geometry, as shown in [10], power allocation can also help reduce the coherence, and thus, improve the radar performance. Therefore, a joint scheme of power allocation and antenna placement can exploit the available DOFs more efficiently. Such an approach was previously considered in [16] where an iterative method was proposed to reduce the required number of TX antennas compared to a conventional sparse MIMO configuration over a given aperture. Nevertheless, our experiments show that the method of [16] fails to converge to a sparse solution (i.e., placement) for moderate to large apertures. Besides, the method is computationally demanding. The power allocation method proposed in [9], can also provide sparse placement if the distance between elements is rather low (compared to wavelength) as it assigns very low powers to some elements. However there is no control on the coherence and the number of antennas in this approach.

In this letter, we provide an efficient solution to the problem of joint antenna placement and power allocation in a CS-based colocated MIMO radar. Our approach is to minimize the number of TX antennas while controlling the recovery quality (and thereby the radar performance) by applying a tunable upper-bound on the coherence of the resulting sensing matrix. Unlike the method of [9],

Corresponding author: A. Ajorloo (e-mail: ajorloo@ee.sharif.edu).1

Associate Editor: Alan Smithee.

This work was supported by Iran National Science Foundation (INSF) under Grant 98010994.

Digital Object Identifier 10.1109/LENS.2017.0000000

the number of TX antennas can be controlled via appropriate tuning of this upper-bound. We formulate the problem as minimizing the ℓ_0 -norm of a selection-power vector with a total power budget constraint on a uniform grid of all possible TX antenna locations. Due to the non-convexity of the ℓ_0 -norm minimization problem, we reformulate the problem as a convex relaxation and recast it as a second order cone program (SOCP) that can be solved efficiently in polynomial time. Using computer experiments, we show the superiority of the proposed method over the existing ones. Especially, we demonstrate that the proposed method, unlike the method of [16], yields sparse placements even for large apertures.

II. SYSTEM MODEL

Consider a colocated MIMO radar system equipped with distinct linear TX and RX arrays placed along the z -axis. The RX array is assumed to be a fixed array which can be of any form such as uniform, co-prime, nested, etc. Here, we consider an N -element uniform linear array (ULA) with $\lambda/2$ inter-element spacing. This array forms an aperture of $L_r = N/2$ if normalized by the wavelength. In the rest of this paper, all reported distances are also normalized in a similar way. The RX steering vector at the DOA parameter $u = \sin \theta$ can be described as

$$\mathbf{b}(u) = [e^{j2\pi z_{r,1}u}, e^{j2\pi z_{r,2}u}, \dots, e^{j2\pi z_{r,N}u}]^T, \quad (1)$$

where $z_{r,n} = \frac{n-1}{2}$, $n = 1, \dots, N$ is the location of the n th receive element on the z -axis. To form the TX array, however, a number of antennas, say M , should be selected from an extended TX array defined over a given aperture L_t . To this end, we consider a uniform grid of possible antenna locations with inter-spacing d across the array. The extended TX array consists of $\tilde{M} = \frac{L_t}{d} + 1$ elements, the steering vector of which at $u = \sin \theta$ is denoted by

$$\tilde{\mathbf{a}}(u) = [e^{j2\pi z_{t,1}u}, e^{j2\pi z_{t,2}u}, \dots, e^{j2\pi z_{t,\tilde{M}}u}]^T \quad (2)$$

where $z_{t,m} = \frac{(m-1)d}{2}$, $m = 1, \dots, \tilde{M}$ denotes the position of the m th element in the extended TX array on the z -axis.

Let us define the selection-power vector as $\mathbf{c} = [c_1, c_2, \dots, c_{\tilde{M}}]^T$, where c_m is a non-negative variable denoting the power of a possibly selected transmit antenna. Indeed, $c_m = 0$ implies that the m th element of the extended TX array is not selected, while a non-zero variable indicates selecting the m th TX antenna with a transmit power equal to c_m . By assuming K targets at the far-field of the radar with DOA parameters u_1, \dots, u_K , the baseband received signal at the n th receiver can be written, in matrix form, as

$$\mathbf{r}_n = \sum_{k=1}^K \beta_k b_n(u_k) \mathbf{X} \mathbf{C} \tilde{\mathbf{a}}(u_k) + \mathbf{n}_n \quad (3)$$

where β_k 's stand for the target reflection coefficients, $b_n(u_k) = e^{j2\pi z_{r,n}u_k}$ is the n th element of $\mathbf{b}(u_k)$ corresponding to the n th receiver, and $\mathbf{X} = [\mathbf{x}_1, \dots, \mathbf{x}_M]$ is the waveform matrix in which \mathbf{x}_i denotes the transmitted signal by the i th TX antenna (it is assumed that $\|\mathbf{x}_i\|_2 = 1$ for all $i = 1, \dots, M$). $\mathbf{C}_{M \times \tilde{M}}$ is the selection-power matrix constructed via removing the all-zero rows in $\text{diag}(\hat{\mathbf{c}})$, where $\hat{\mathbf{c}}$ denotes the element-wise square root of \mathbf{c} (we have $\mathbf{C}^H \mathbf{C} = \text{diag}(\hat{\mathbf{c}})$). The vector \mathbf{n}_n denotes the noise term at the n th receiver which is modeled as a circularly symmetric complex Gaussian random vector.

At a processing unit, the received vectors corresponding to all the receivers are stacked together to form the total received signal

$$\mathbf{r} = [\mathbf{r}_1^T, \dots, \mathbf{r}_N^T]^T = \sum_{k=1}^K \beta_k \mathbf{b}(u_k) \otimes \mathbf{X} \mathbf{C} \tilde{\mathbf{a}}(u_k) + \mathbf{n} \quad (4)$$

where \otimes is the Kronecker product operator and $\mathbf{n} = [\mathbf{n}_1^T, \dots, \mathbf{n}_N^T]^T$ is the total noise vector.

Next, we present the aforementioned model in a grid-based formulation in a CS framework. To this end, let us assume a fine-enough uniform grid g_1, \dots, g_G for the possible DOA parameters, where G is the size of the grid ($G \gg K$). Further, we assume that the observed direction of all the targets in the surveillance area fairly lie on the grid points. Hence, we can write the received vector \mathbf{r} in a CS framework as

$$\mathbf{r} = \Phi \mathbf{s} + \mathbf{n} \quad (5)$$

where $\Phi = [\boldsymbol{\varphi}_1, \boldsymbol{\varphi}_2, \dots, \boldsymbol{\varphi}_G]$ is the sensing matrix whose l th column (associated with the l th DOA grid point g_l) can be written as

$$\boldsymbol{\varphi}_l = \mathbf{b}(g_l) \otimes \mathbf{X} \mathbf{C} \tilde{\mathbf{a}}(g_l), \quad l = 1, \dots, G, \quad (6)$$

and \mathbf{s} is a sparse vector, the l th element of which is equal to β_k if the k th target lies in the l th DOA bin (g_l) and is zero otherwise. To detect and estimate existing targets, we need to recover \mathbf{s} from the measurements \mathbf{r} in (5) via a sparse recovery method. We employ the NESTA recovery algorithm presented in [17] which is an appropriate technique for complex-valued vectors and matrices. To decide about the presence of a target in a DOA bin, the magnitude of the corresponding element in the recovered vector \mathbf{s} is compared with a given threshold; the value of the threshold is determined based on a desired false alarm probability.

III. PROPOSED METHOD

The task of joint antenna placement and power allocation is performed with the aim of minimizing the number of TX antennas, which can be formulated as minimizing the number of nonzero elements in \mathbf{c} . We further upper-bound the coherence of the sensing matrix to control the sparse recovery accuracy, and thus the detection performance of the MIMO radar. Mathematically, we consider the following constrained minimization problem

$$\min_{\mathbf{c}} \|\mathbf{c}\|_0 \quad \text{s.t.} \begin{cases} \mu(\Phi) \leq \eta, \\ \sum_{m=1}^{\tilde{M}} c_m = P_T, \quad \mathbf{c} \geq \mathbf{0} \end{cases}, \quad (7)$$

where P_T denotes the total power budget and $\mu(\Phi)$ stands for the coherence of the sensing matrix Φ defined as

$$\mu(\Phi) = \max_{l \neq l'} \frac{|\boldsymbol{\varphi}_l^H \boldsymbol{\varphi}_{l'}|}{\|\boldsymbol{\varphi}_l\| \|\boldsymbol{\varphi}_{l'}\|}, \quad (8)$$

where $\boldsymbol{\varphi}_l$ is defined in (6). Furthermore, the design parameter η is a constant which sets an upper-bound on the coherence. In the rest of the paper, we consider orthogonal radar waveforms, i.e., $\mathbf{X}^H \mathbf{X} = \mathbf{I}$. Furthermore, we denote the vectors $\tilde{\mathbf{a}}(g_l)$ and $\mathbf{b}(g_l)$ by $\tilde{\mathbf{a}}_l$ and \mathbf{b}_l for the sake of brevity. According to (6), and using some properties of the Kronecker product, the expression $|\boldsymbol{\varphi}_l^H \boldsymbol{\varphi}_{l'}|$ in the coherence formulation can be simplified as

$$|\boldsymbol{\varphi}_l^H \boldsymbol{\varphi}_{l'}| = b_{l,l'} |\text{Tr}\{\mathbf{A}_{l,l'} \text{diag}(\mathbf{c})\}| \quad (9)$$

where $b_{l,l'} \triangleq |\mathbf{b}_l^H \mathbf{b}_{l'}|$, $\mathbf{A}_{l,l'} \triangleq \tilde{\mathbf{a}}_l \tilde{\mathbf{a}}_{l'}^H$, and we used the relation $\mathbf{C}^H \mathbf{C} = \text{diag}(\mathbf{c})$ and a property of $\text{Tr}\{*\}$ operator. Finally, one can simplify the expression as

$$\boldsymbol{\varphi}_{l'}^H \boldsymbol{\varphi}_l = b_{l,l'} |\mathbf{c}^T \mathbf{a}_{l,l'}|, \quad (10)$$

where $\mathbf{a}_{l,l'} \triangleq \text{diag}(\mathbf{A}_{l,l'})$ is the vector on the main diagonal in $\mathbf{A}_{l,l'}$. Furthermore, for $l = l'$ we have $\boldsymbol{\varphi}_l^H \boldsymbol{\varphi}_l = \|\boldsymbol{\varphi}_l\|^2 = N \sum_{m=1}^{\tilde{M}} c_m$.

By recalling that $\mathbf{A}_{l,l'}$ and $b_{l,l'}$ are solely dependent on the difference of the indices l and l' , we can simplify the coherence expression in (8) as

$$\mu(\Phi) = \max_{l=2,3,\dots,G} \frac{b_{l,1} |\mathbf{c}^T \mathbf{a}_{l,1}|}{N \sum_{m=1}^{\tilde{M}} c_m}. \quad (11)$$

Now consider putting (11) into (7); the resulting problem is still computationally difficult to solve due to the existence of ℓ_0 -norm in the objective function. Therefore, we use the ℓ_1 -norm as a convex relaxation of the ℓ_0 -norm. However, this substitution is not directly compatible with the total power budget constraint ($\sum_{m=1}^{\tilde{M}} c_m = P_T$); indeed, as c_i s are non-negative we know that $\|\mathbf{c}\|_1 = \sum_{m=1}^{\tilde{M}} c_m$. We should highlight that both the objective function and the coherence constraint are invariant to scaling of \mathbf{c} . Thus, we can simply remove the total power constraint and satisfy it later via an appropriate scaling. With the latter change, we write the corresponding ℓ_1 -norm minimization problem as the following convex form:

$$\min_{\mathbf{c}} \|\mathbf{c}\|_1 \quad \text{s.t.} \begin{cases} b_{l,1} |\mathbf{c}^T \mathbf{a}_{l,1}| \leq \eta N \sum_{m=1}^{\tilde{M}} c_m, & l = 2, \dots, G \\ \mathbf{c} \geq \mathbf{0}. \end{cases} \quad (12)$$

Unfortunately, $\mathbf{c} = \mathbf{0}$ is the trivial solution of (12). To avoid this solution, we need to guarantee that at least one of the c_i s is non-zero. Due to the aforementioned scaling-invariance property of the minimization problem, this non-zero c_i can be set as 1 without loss of generality (other c_i s shall be scaled accordingly). In case the index i for a non-zero value is known, we can simply solve the following second order cone program (SOCP)

$$\min_{\mathbf{c}} \mathbf{1}^T \mathbf{c} \quad \text{s.t.} \begin{cases} |\mathbf{c}^T \mathbf{a}_{l,1}| \leq \frac{\eta N}{b_{l,1}} \mathbf{1}^T \mathbf{c}, & l = 2, \dots, G \\ c_i = 1, & \mathbf{c} \geq \mathbf{0}. \end{cases} \quad (13)$$

The above SOCP can be efficiently solved using off-the-shelve packages such as CVX. Since the index of a non-zero element (alternatively, the location of an existing antenna) is not known a priori, we solve (13) for all $i = 1, \dots, \tilde{M}$ and select the sparsest solution. Due to the symmetry of the problem, it is not difficult to check that the solution for i and $\tilde{M} - i$ are equivalent. Hence, checking the range $i = 1, \dots, \lceil \frac{\tilde{M}}{2} \rceil$ suffices to find the sparsest solution.

Remark 1: As it is known, the angular resolution of a MIMO radar is inversely proportional to the aperture of the virtual array which equals the sum of the TX and the RX apertures ($L_v = L_t + L_r$). More precisely, the resolution in $u = \sin \theta$ domain equals $1/L_v$. For detection purposes in radar systems, typically one to two samples are observed in each resolution cell. Here, we consider a uniform grid of $\frac{2}{3L_v}$ -spaced for the u parameter over the entire visible region $[-1, 1]$; this is equivalent to taking three samples from each two cells.

Remark 2: In the proposed method, the RX array with N receivers is a fixed ULA with aperture $L_r = N/2$. The TX aperture L_t , however, is given as an input to the proposed method.

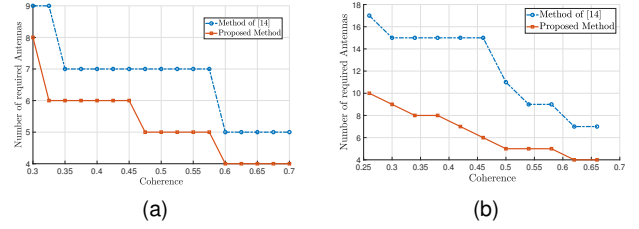


Fig. 1. Required number of TX antennas versus coherence, (a) $N = 5$, $L_t = 20$, (b) $N = 10$, $L_t = 55$.

IV. SIMULATION RESULTS

In this section, we aim at comparing the proposed method with the existing methods and especially with the method of [16] using computer experiments. In the first experiment, we consider a standard ULA with $N = 5$ receiving antennas; it provides us with an RX aperture of $L_r = 5/2$. Further, we set $L_t = 20$ and $d = 1/2$. Under these settings, we run the proposed method and the method of [16] for different coherence values and report the required number of TX antennas for each. The results are shown in Fig. 1a. As shown in this figure, the proposed scheme requires fewer antennas and results in sparser arrays, and thus is more cost-effective. We did the same experiment using $N = 10$ and $L_t = 55$ and plotted the results in Fig. 1b. It is observed in this figure that for larger apertures, the method of [16] does not exhibit good performances and the superiority of our scheme is further emphasized under these circumstances. In fact, as the aperture increases, the iterative method of [16] somehow fails to find a sparse solution. This observation is confirmed by checking the resulting locations and powers (Fig. 2). The results for both methods for a coherence values of 0.38 are given in Fig. 2a and Fig. 2b and for a coherence value of 0.5 in Fig. 2c and Fig. 2d. As mentioned, we see that the method of [16] has not converged to a sparse solution. Particularly, if we discard the antenna with the least allocated (nonzero) power in Fig. 2c, the coherence is increased by 10% which is not negligible.

In the previous experiment, the reduction of the TX antennas in the proposed scheme compared to [16] was reported. In the following experiment, we evaluate our method in terms of the detection performance. Indeed, due to the dependence of the sparse recovery performance on the coherence, it is expected that methods perform similarly under equal coherence values. To examine this, we compare our design shown in Fig. 2d with 5 TX antennas with that of [16] shown in Fig 2c with 11 TX antennas (employing the same setup used in generating the curves of Fig. 1b); the coherence value in both arrangements is 0.5. We also include the results of an arrangement with 10 TX antennas and a coherence value of 0.26 using the proposed method, as well as a configuration with 10 TX elements obtained via performing the power allocation method proposed by [9] over a TX aperture of size $L_t = 45$; the coherence of the latter is 0.54. Note that in all of the designs, the RX array is a standard ULA with $N = 10$ antennas. we generate the curves of detection probability as a function of signal to noise ratio (SNR) for a given false alarm probability P_{fa} via a Monte-Carlo simulation. Here, SNR is defined as $1/\sigma^2$ where σ^2 is the power of complex Gaussian noise at the receiver. We consider a 2500-trial Monte-Carlo simulation with independent realizations of noise, target locations and target gains. Furthermore, we employ orthonormal DFT matrices as the waveform matrix \mathbf{X} .

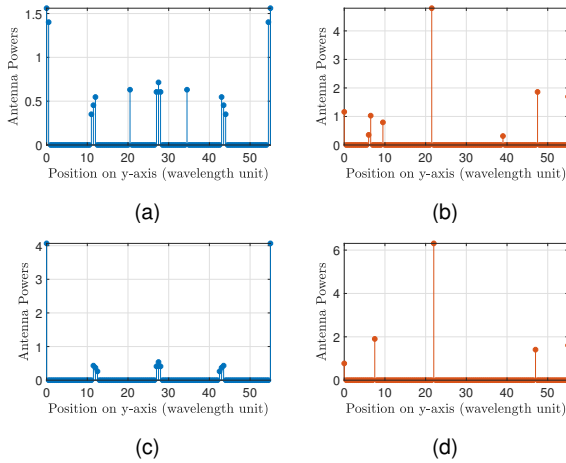


Fig. 2. Position and power of the selected antennas, (a) method of [16], coherence = 0.38, (b) proposed method, coherence = 0.38 (c) method of [16], coherence = 0.5, (d) proposed method, coherence = 0.5.

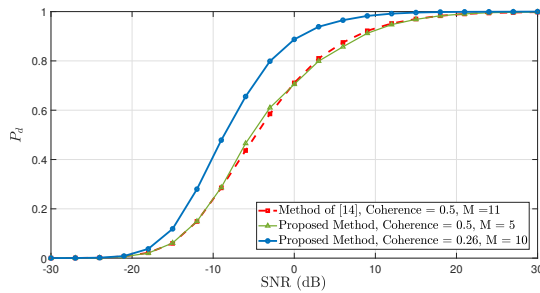


Fig. 3. Probability of detection versus SNR, $P_{fa} = 10^{-4}$, $K = 4$

In each ensemble run, we randomly place $K = 4$ targets on the DOA grid points with random reflection coefficients (β_k 's) following a Swerling case I model. In other words, β_k 's follow a standard complex Gaussian distribution. Then, we form the noisy measurements using the CS expression (5) and attempt to recover the target scene (the vector \mathbf{s}) using NESTA [17]. Next, we perform a detection procedure by comparing the recovered data with a threshold computed according to the given value of $P_{fa} = 10^{-4}$. The resulting curves are given in Fig. 3. As shown in this figure, our design with 10 TX elements significantly outperforms the designs using the methods of [16] and [9] with 11 and 10 TX elements, respectively. Further, for the same coherence value of 0.5, the resulting MIMO configuration obtained via the proposed scheme with only 5 TX antennas provides a detection performance very close to that of the [16] with 11 TX antennas.

As a last experiment, we compare our schemes with that of [16] in terms of computational time. For a fixed number of RX antennas ($N = 6$), we extracted the run time of the algorithms over our machine for different values of L_t . The results are shown in Fig. IV, indicating that the proposed method is much faster than the iterative method of [16].

V. CONCLUSION

A joint scheme of antenna placement and power allocation in CS-based colocated MIMO radars was proposed in this letter. Our method was based on the minimization of the ℓ_1 -norm of a selection-power vector defined over a uniform grid of possible locations for

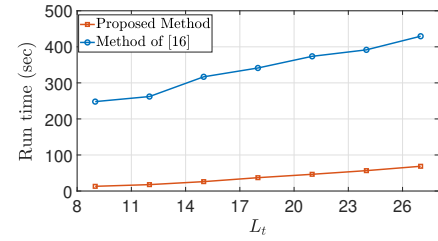


Fig. 4. Run time vs L_t , $N = 6$

antennas. The superiority of the proposed method over the existing methods was shown by numerical simulations. As an extension to our work, the problem could be formulated for continuous location variables while taking into account some physical constraints such as minimum antenna spacing. Furthermore, as a general scenario, the inclusion of non-orthogonal waveforms could also be considered; especially since it paves the way for beam-pattern design.

REFERENCES

- [1] J. Li and P. Stoica, "MIMO radar with colocated antennas," *IEEE Signal Processing Magazine*, vol. 24, no. 5, pp. 106–114, 2007.
- [2] A. M. Haimovich, R. S. Blum, and L. J. Cimini, "MIMO radar with widely separated antennas," *IEEE Signal Processing Magazine*, vol. 25, no. 1, pp. 116–129, 2008.
- [3] Y. Yu, A. P. Petropulu, and H. V. Poor, "MIMO radar using compressive sampling," *IEEE Journal of Selected Topics in Signal Processing*, vol. 4, no. 1, pp. 146–163, 2010.
- [4] C.-Y. Chen and P. Vaidyanathan, "Compressed sensing in MIMO radar," in *2008 42nd Asilomar Conference on Signals, Systems and Computers*. IEEE, 2008, pp. 41–44.
- [5] E. J. Candes, "The restricted isometry property and its implications for compressed sensing," *Comptes Rendus Mathématique*, vol. 346, no. 9–10, pp. 589–592, 2008.
- [6] A. Ajourloo, R. Amiri, M. Bastani, and A. Amini, "Sensor selection for sparse source detection in planar arrays," *Electronics Letters*, vol. 55, no. 7, pp. 411–413, 2019.
- [7] T. Strohmer and H. Wang, "Accurate imaging of moving targets via random sensor arrays and Kerdock codes," *Inverse Problems*, vol. 29, no. 8, p. 085001, 2013.
- [8] Y. Yu, A. P. Petropulu, and H. V. Poor, "Power allocation for cs-based colocated mimo radar systems," in *2012 IEEE 7th Sensor Array and Multichannel Signal Processing Workshop (SAM)*. IEEE, 2012, pp. 217–220.
- [9] Y. Yu, S. Sun, R. N. Madan, and A. Petropulu, "Power allocation and waveform design for the compressive sensing based MIMO radar," *IEEE Transactions on Aerospace and Electronic Systems*, vol. 50, no. 2, pp. 898–909, 2014.
- [10] A. Ajourloo, A. Amini, and M. H. Bastani, "An approach to power allocation in MIMO radar with sparse modeling for coherence minimization," in *2017 25th European Signal Processing Conference (EUSIPCO)*, Aug 2017, pp. 1927–1931.
- [11] A. Ajourloo, A. Amini, and M. H. Bastani, "A compressive sensing-based colocated MIMO radar power allocation and waveform design," *IEEE Sensors Journal*, vol. 18, no. 22, pp. 9420–9429, 2018.
- [12] P. Gong, W.-Q. Wang, F. Li, and H. C. So, "Sparsity-aware transmit beamspace design for FDA-MIMO radar," *Signal Processing*, vol. 144, pp. 99–103, 2018.
- [13] A. Ajourloo, A. Amini, E. Tohidi, M. H. Bastani, and G. Leus, "Antenna placement in a compressive sensing based colocated MIMO radar," *IEEE Transactions on Aerospace and Electronic Systems*, pp. 1–1, 2020.
- [14] M. Rossi, A. M. Haimovich, and Y. C. Eldar, "Spatial compressive sensing for MIMO radar," *IEEE Transactions on Signal Processing*, vol. 62, no. 2, pp. 419–430, Jan 2014.
- [15] A. Harlakin, J. Mietzner, P. A. Hoeher, and A. Meusling, "Compressive-sensing-aided mimo radar enabling multi-functional and compact sensors in air scenarios using optimized antenna arrays," *IEEE Access*, vol. 9, pp. 41 417–41 429, 2021.
- [16] A. Ajourloo, A. Amini, and M. H. Bastani, "Compressive sensing-based colocated MIMO radar with reduced number of transmit antennas," in *2019 Iran Workshop on Communication and Information Theory (IWCIT)*. IEEE, 2019, pp. 1–6.
- [17] S. Becker, J. Bobin, and E. J. Candès, "NESTA: A fast and accurate first-order method for sparse recovery," *SIAM Journal on Imaging Sciences*, vol. 4, no. 1, pp. 1–39, 2011.